THE JOURNAL OF CHEMICAL PHYSICS **133**, 164508 (2010)

Polarized Raman spectroscopic study of relaxed high density amorphous ices under pressure

Yoshiharu Suzuki[1,a)] and Yasunori Tominaga[2]
[1]*National Institute for Materials Science, Namiki 1-1, Tsukuba, Ibaraki 305-0044, Japan*
[2]*Ochanomizu University, Ootsuka 2-1-1, Bunkyo, Tokyo 112-8610, Japan*

(Received 18 June 2010; accepted 2 October 2010; published online 25 October 2010)

We have made high density amorphous ice (HDA) by the pressure-induced amorphization of hexagonal ice at 77 K and measured the volume change on isobaric heating in a pressure range between 0.1 and 1.5 GPa. The volume of HDA on heating below ~0.35 GPa increases, while the volume of HDA on heating above ~0.35 GPa decreases. The polarized OH-stretching Raman spectra of the relaxed HDAs are compared with that of the unannealed HDA. The relaxed HDAs are prepared at 0.2 GPa at 130 K and 1.5 GPa at 160 K. It is found that the relatively strong totally symmetric OH-stretching vibration mode around 3100 cm^{-1} exists in the depolarized reduced Raman spectrum χ''_{VH} of the unannealed HDA and that its intensity rapidly decreases by relaxation. The χ''_{VH} profiles of the relaxed HDA are similar to those of liquid water. These results indicate that the HDA reaches a nearly equilibrium state by annealing and the intrinsic state of HDA relates to a liquid state. The pressure-volume curve of the relaxed HDA at 140 K seems to be smooth in the pressure range below 1.5 GPa. © *2010 American Institute of Physics*. [doi:10.1063/1.3505045]

I. INTRODUCTION

In order to explain the mystery of liquid water at low temperatures, the theoretical and experimental studies relating to water polyamorphism, the liquid-liquid phase separation of liquid water, and the second critical point theory of water are advancing apace.[1–3] However, the direct observation of the liquid-liquid phase separation and/or the second critical point in the deeply supercooled regions is difficult because of extremely rapid crystallization of liquid water. According to the scenario of water polyamorphism,[1] low-density liquid (LDL) and high density liquid (HDL) correspond to low-density amorphous ice (LDA) and high density amorphous ice (HDA), respectively. Therefore, the understanding of water polyamorphism is based on the indirect information obtained from measurements of these amorphous ices. For example, giving abundant evidences of the first order nature of LDA-HDA phase transition and the thermodynamical connectivity between HDA and HDL (or liquid water under high pressure) experimentally is the key that verifies the validity of water polyamorphism.

Recently, another high density amorphous phase which is denser than HDA, so-called very high density amorphous ice (VHDA), has been reported.[4] In order to clarify the difference or similarity between HDA and VHDA, the structures of HDA and VHDA[5–11] and the thermodynamical properties of HDA and VHDA[12–14] are probed. On the other hand, static and dynamical structures of HDA in the vicinity of a coexistence line of HDA and LDA are examined closely.[15–18] However, the experiments of HDA at low temperatures are always carried out under nonequilibrium condition. Because of the high viscosity of HDA, the relaxation of HDA is extremely slow and the deformation does not catch up with the change of external field. We notice that the pressure-induced densification relating to the slow relaxation is observed in a general glassy system and that this phenomena causes confusion to the understanding of polyamorphism.[19] Therefore, we are conscious that the experimental information on amorphous ices at low temperatures depends strongly on experimental methods and sample conditions and we should pay close attention for evaluating the experimental data of amorphous ices.

In the present paper, in order to understand the HDA in an equilibrium state, we measure the volume of HDA on isobaric heating in a pressure range between 0.1 and 1.5 GPa and examine the annealing effect on the change of HDA state using a polarized Raman spectroscopy. This study deepens not only the understanding of water polyamorphism but also the understanding of the structural relaxation of glassy materials under nonequilibrium.

II. EXPERIMENTAL AND ANALYSIS METHOD

The initial HDA sample is made by the pressure-induced amorphization of crystalline ice I_h at 77 K. An indium container, in which ultrapure liquid water (H_2O) of about 1.5 cm^3 is completely sealed up, is placed in a piston-cylinder pressure device to which a heater and thermocouples are attached. The diameter of the piston is 15 mm. The pressure device is cooled at 77 K by cold nitrogen gas. In order to avoid rapid generation of heat which is accompanied with phase transition, the sample is compressed at a compression ratio lower than 0.15 GPa min^{-1}. The amorphization of ice I_h begins to occur at ~1.2 GPa and in order to complete the amorphization, the sample is compressed further up to ~1.5 GPa and is kept at 1.5 GPa for 10 min.

[a)] Electronic mail: suzuki.yoshiharu@nims.go.jp.

The absolute and relative errors of the correct sample pressure are ±~0.01 and ±~0.005 GPa, respectively. The sample temperature error is ±~2 K.

HDA sample is decompressed directly from 1.5 GPa to a given pressure in a pressure range between 0.1 and 1.5 GPa at a decompression ratio lower than 0.15 GPa min^{-1} and heated from 77 to 230 K at 0.3 K s^{-1}. The displacement of piston is recorded during the heating. In order to calculate the specific volume of HDA, we carry out volumetric measurements of only the indium container on isobaric heating independently and subtract the volume of the indium container from the volume of both HDA sample and the indium container. The volume is accurate to within 1.0%.

The polarized Raman spectra in the OH-stretching region from 2800 to 3800 cm^{-1} are measured by using microscope Raman spectroscopy (Jobin Yvon T-64000). The resolution of the Raman spectrum is about 0.1 cm^{-1}. The incident laser is argon ion laser with a wavelength of 488.0 nm and a power of 500 mW at the source. The intensity of the Raman scattered radiation polarized parallel to the incident light I_{VV} and the intensity of the Raman scattered radiation polarized perpendicular to the incident light I_{VH} are measured separately. The scattered volume of the HDA sample for I_{VV} and I_{VH} are the same.

The intensity of all the recorded Raman spectra is corrected by polarizer characteristics and background function. The corrected intensity is converted into the imaginary part of dynamical susceptibility as follows:

$$\chi''(\nu) = \frac{\kappa}{(\nu_L - \nu)^3}\left(1 - \exp\left(-\frac{hc\nu}{k_B T}\right)\right)\mathrm{I}(\nu).$$

ν stands for the Raman-shifted frequency written by cm^{-1} which is defined as $\nu = f/c$, where f is the frequency in hertz and c is the velocity of light. ν_L is the incident laser frequency written by cm^{-1}, h is Planck's constant, k_B is Boltzmann's constant, and T is the absolute temperature. K is the instrumental constant and is fixed to be unity.

In order to discuss the OH-stretching vibrational Raman spectra quantitatively, Raman spectra are analyzed by a linear combination of three or four Gaussian functions $[g(\nu)]$ as follows:

$$\chi''(\nu) = \sum_{n=1}^{3\text{ or }4} g_n(\nu) = \sum_{n=1}^{3\text{ or }4} A_n \exp\left(\frac{-(\nu - \nu_n)^2}{\gamma_n^2}\right),$$

where A_n is the amplitude, ν_n is the central frequency, and γ_n is the distribution. The HDA specimen which is recovered from high pressure to ambient pressure at 77 K is set in a cryostat and the Raman spectra are measured at 35 K at 1 atm.

III. RESULTS AND DISCUSSIONS

The volume changes of HDA on isobaric heating are shown in Fig. 1. The pattern of the temperature dependence of the volume changes at ~0.35 GPa. Above ~0.35 GPa, the volume of HDA decreases continuously with increasing temperature and when the temperature is raised further, the volume decreases rapidly and discontinuously. This discontinuous volume change represents the crystallization to high-pressure crystalline ice. On the contrary, the volume of HDA on isobaric heating below ~0.35 GPa increases continuously with increasing temperature. When the temperature is raised further, the HDA crystallizes accompanied with discontinuous volume increase. The crystallization temperature T_x and the crystalline formation depend on the heating ratio and pressure.[20] The continuous volume change of the unannealed HDA by the first heating before the crystallization is irreversible.

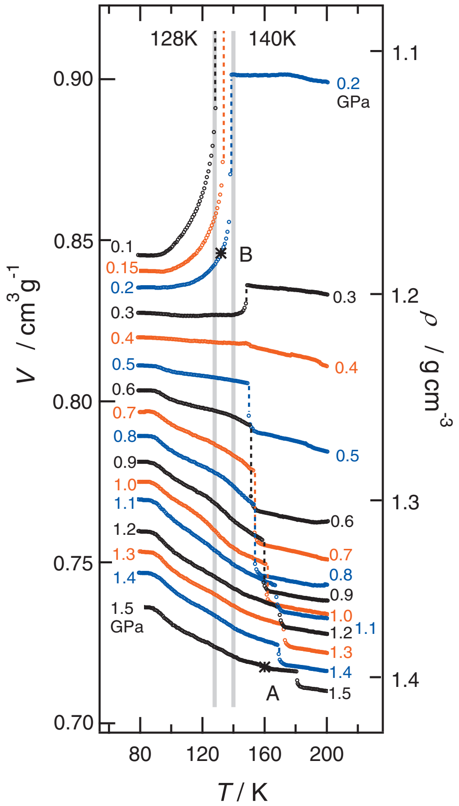

FIG. 1. Volume changes of HDA on isobaric heating in the pressure range between 0.1 and 1.5 GPa. The broken lines denote the crystallization. Asterisks A and B stand for the volume of the 1.5 GPa-relaxed HDA and the volume of the 0.2 GPa-relaxed HDA, respectively. We believe that there is little effect of microcrack (Ref. 7) on the volume measurements during the decompression down to 0.1 GPa since the creation of microcrack occur near 1 atm.

In Fig. 2, the onset of T_x is plotted as the function of pressure. With increasing pressure T_x becomes higher. The pressure dependence of T_x below 1.5 GPa is consistent with the results in Refs. 20 and 21. When HDA is compressed up to ~4 GPa at 77 K, it crystallizes to ice VII′.[22] Therefore, it is assumed that the value of T_x may become the maximum somewhere between 1.5 and 4 GPa.[21]

Now, in order to examine the differences among the HDA densified by heating at higher pressure, the HDA expanded by heating at lower pressure and the unannealed HDA, we prepare two kinds of relaxed HDA. One is a densified HDA which is heated at 1.5 GPa at 160 K, which is slightly below its T_x (point A in Fig. 1 and process 1 in Fig. 2), and is referred to as "the 1.5 GPa-relaxed HDA." Another is an expanded HDA which is relaxed at 0.2 GPa at 130 K, which is slightly below its T_x (point B in Fig. 1 and process 2 in Fig. 2), and is referred to as "the 0.2 GPa-relaxed HDA."

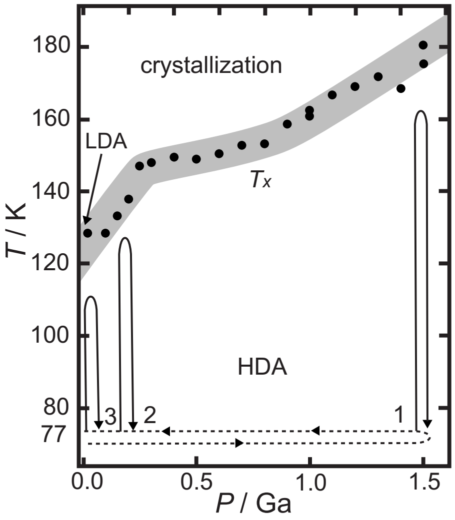

FIG. 2. Pressure dependence of T_x and annealing process of unannealed HDA. Value of T_x is estimated from volume change of HDA on isobaric heating in Fig. 1. Processes 1, 2, and 3 are the isobaric heating processes at 1.5 GPa–160 K, at 0.2 GPa–130 K, and at 1 atm–110 K, respectively.

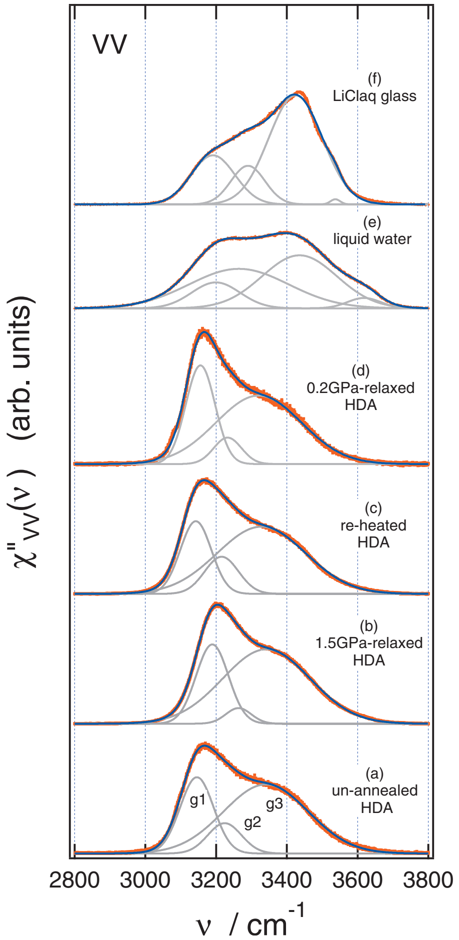

FIG. 3. Polarized (VV) reduced Raman spectra for several kinds of HDA, liquid water, and glassy LiCl aqueous solution in the OH-stretching region. (a) The unannealed HDA. (b) The 1.5 GPa-relaxed HDA. (c) The reheated HDA. (d) The 0.2 GPa-relaxed HDA. (e) Liquid water measured at 1 atm at 280 K. (f) Glassy LiCl aqueous solution of 14.3 mol % (R=6). This glassy solution is vitrified by cooling from room temperature to 77 K at 1 atm and is measured at 1 atm at 35 K. Red dots denote the measured Raman spectra χ''_{VV}. Blue spectra are results analyzed by a linear combination of some Gaussian functions (gray lines).

From a visual observation of the recovered HDA samples, the unannealed HDA is opaque and very fragile solid. In contrast to the unannealed HDA, it is recognized that some transparent and rigid blocks are formed in the 1.5 GPa-relaxed HDA and the 0.2 GPa-relaxed HDA.

The polarized reduced Raman spectra in OH-stretching region, χ''_{VV} and χ''_{VH}, of the unannealed HDA, the 1.5 GPa-relaxed HDA and the 0.2 GPa-relaxed HDA are shown in Figs. 3 and 4, respectively. The lowest component $g_1(\nu)$ of χ''_{VV} and χ''_{VH} of the 1.5 GPa-relaxed HDA [Figs. 3(b) and 4(b)] shift to higher frequency side than those of the unannealed HDA [Figs. 3(a) and 4(a)] by about 35 cm^{-1}. However, the whole spectral profile of the χ''_{VV} of the 1.5 GPa-relaxed HDA is similar to that of the unannealed HDA. On the contrary, the χ''_{VH} profile of the 1.5 GPa-relaxed HDA [Fig. 4(b)] is remarkably different from that of the unannealed HDA [Fig. 4(a)]. The most characteristic differences between these χ''_{VH} profiles are that a relatively strong $g_1(\nu)$ mode around 3100 cm^{-1} exists in the χ''_{VH} of the unannealed HDA and that this $g_1(\nu)$ mode becomes extremely small by annealing. In order to quantify the decrease of the $g_1(\nu)$ mode, we estimate a depolarization ratio of $g_1(\nu)$ mode, $\sigma_1(=A_1$ of χ''_{VH}/A_1 of $\chi''_{\mathrm{VV}})$. The σ_1 of 1.5 GPa-relaxed HDA is 0.030 and the σ_1 of the unannealed HDA is 0.158.

Next, the 1.5 GPa-relaxed HDA is heated up to 110 K at 1 atm (process 3 in Fig. 2) and is expanded up to almost the same volume of the unannealed HDA. The χ''_{VV} of this reheated HDA [Fig. 3(c)] shifts toward the lower frequency side than the χ''_{VV} of the 1.5 GPa-relaxed HDA and the peak position almost coincides with that of the initial unannealed HDA. However, the χ''_{VH} profile of the reheated HDA changes little from the χ''_{VH} profile of the 1.5 GPa-relaxed HDA and its $g_1(\nu)$ mode is small. The σ_1 of the reheated HDA is 0.025 and is nearly equal to the σ_1 of the 1.5 GPa-relaxed HDA (0.030). This indicates that though the position shift of Raman spectra is caused by the change in volume, the change in the amplitude of $g_1(\nu)$ mode in the χ''_{VH} is irrelevant to the change of both intermolecular distance and bond strength between water molecules.

Though the χ''_{VV} profile of the 0.2 GPa-relaxed HDA [Fig. 3(d)] is similar to that of the unannealed HDA, the χ''_{VH} profile of the 0.2 GPa-relaxed HDA [Fig. 4(d)] is different from that of the unannealed HDA. Rather, the χ''_{VH} profile of the 0.2 GPa-relaxed HDA is similar to that of the 1.5 GPa-relaxed HDA. The σ_1 of the 0.2 GPa-relaxed HDA is 0.067. It is pronouncedly smaller than the σ_1 of the unannealed HDA and is slightly larger than the σ_1 of the 1.5 GPa-relaxed HDA. Although the isobaric volume changes of the 1.5 GPa-relaxed HDA and the 0.2 GPa-relaxed HDA show an opposite tendency, the changes of the χ''_{VH} profile induced by heating show similar tendency.

The χ''_{VV} and χ''_{VH} of liquid water, which are measured at 280 K at 1 atm and are analyzed by a linear combination of four Gaussian functions, are shown in Figs. 3(e) and 4(e), respectively. In the case of liquid water, the $g_1(\nu)$ mode is identified as the totally symmetric OH-stretching vibration

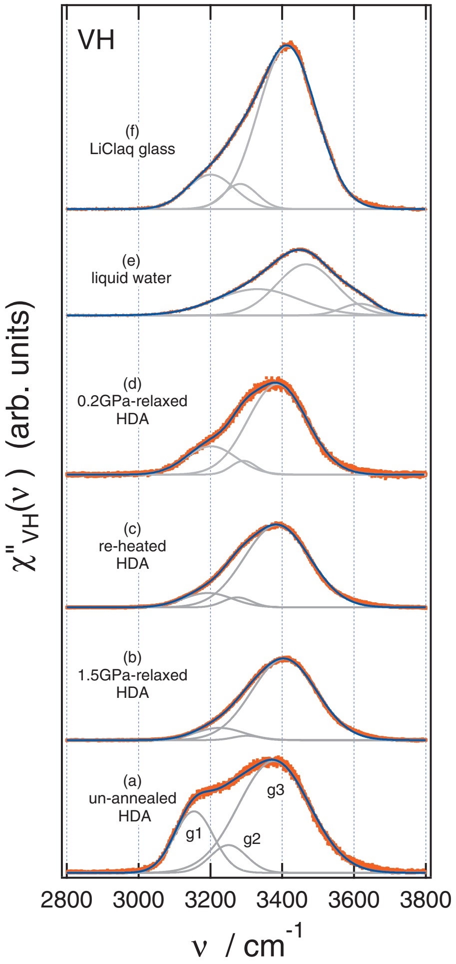

FIG. 4. Depolarized (VH) reduced Raman spectra for several kinds of HDA, liquid water, and glassy LiCl aqueous solution in the OH-stretching region. (a) The unannealed HDA. (b) The 1.5 GPa-relaxed HDA. (c) The reheated HDA. (d) The 0.2 GPa-relaxed HDA. (e) Liquid water measured at 1 atm at 280 K. (f) Glassy LiCl aqueous solution of 14.3 mol % (R=6). Red dots denote the measured Raman spectra χ''_{VH}. Blue spectra are results analyzed by a linear combination of some Gaussian functions (gray lines).

mode and the $g_1(\nu)$ mode in the χ''_{VH} is extremely smaller than the $g_1(\nu)$ mode in the χ''_{VV}.[23] In the present study, the σ_1 of liquid water is 0.020. A similar relation between the $g_1(\nu)$ mode in χ''_{VV} and the $g_1(\nu)$ mode in χ''_{VH} is observed in the Raman spectra detected from glassy lithium chloride (LiCl) aqueous solution of 14.3 mol % (R=6, where R stands for the number of water moles per mole of LiCl) as shown in Figs. 3(f) and 4(f). The σ_1 of the glassy LiCl aqueous solution is 0.070. Though the LiCl aqueous solution vitrified by cooling is under nonequilibrium condition, its glassy state should be in a homogeneously disordered state because of inheritance of liquid state just before the vitrification.

The 1.5 GPa-relaxed HDA in this study corresponds to VHDA.[4] The recent studies on the structure of VHDA show that VHDA is more homogeneously disordered than the unannealed HDA.[9,10] Usually, when a polarized Raman spectrum is measured from a disordered system such as a liquid, the totally symmetric vibration modes in its depolarized Raman spectrum is very small because of preservation of the symmetry of vibration.[24] Actually, the $g_1(\nu)$ modes in the χ''_{VH} of liquid water and glassy LiCl aqueous solution, which are homogeneous disordered systems, are very small, as shown in Figs. 4(e) and 4(f), and this result consists with above theoretical expectation. Therefore, we consider that the decrease of $g_1(\nu)$ mode in the χ''_{VH} of the unannealed HDA by heating may be induced by the structural change that the inhomogeneous molecular configuration frozen in the unannealed HDA relaxes by heating and then the molecular configuration rearranges to be homogeneously disordered. For the same reason, the 0.2 GPa-relaxed HDA may be regarded as homogeneously disordered HDA, though the volume of HDA increases by heating at 0.2 GPa.

The disordered system made by pressure-induced amorphization under nonequilibrium condition should be different intrinsically from the disordered system such as a glassy solution made by cooling of the liquid solution under equilibrium condition. Perhaps the macroscopic structural inhomogeneity, such as locally frozen stress, inhomogeneity of density, partial deformation of hydrogen-bonded networks and so on, might remain in the unannealed HDA because of the nonequilibrium. We consider that these structural inhomogeneities may induce the distortion of the symmetry of totally symmetric vibration mode in the unannealed HDA and as a result, the $g_1(\nu)$ mode in the χ''_{VH} of the unannealed HDA may become large. Namely, the $g_1(\nu)$ mode in the χ''_{VH} may relate closely to an inhomogeneity of the disordered molecular configuration in HDA.

When the 1.5 GPa-relaxed HDA is reheated at 1 atm, there is little change of the $g_1(\nu)$ mode and the intensity of $g_1(\nu)$ is small as shown in Fig. 4(c). This suggests that the reheated HDA is homogeneously disordered. This result seems to be contradictory to the report by Koza *et al.*[8,11] that the nanosized heterogeneity has been formed in the VHDA by annealing at 1 atm. We speculate that the generation of nanosized heterogeneity in VHDA may relate to the density fluctuation induced by a spinodal decomposition relating to HDA and LDA. This nanosized heterogeneity may be undetected by Raman measurement because the $g_1(\nu)$ mode is extremely sensitive to the change of the macroscopic hydrogen-bonded network structure. The important fact in this experimental result is that the χ''_{VH} profile of the reheated HDA is similar to that the 1.5 GPa-relaxed HDA as well as of liquid water, even if the nanosized heterogeneity exists in the reheated HDA.

The χ''_{VV} and χ''_{VH} of LDA made by heating of the 1.5 GPa-relaxed HDA at 1 atm are shown in Fig. 5(a). The existence of a small but pronounced $g_1(\nu)$ mode in the χ''_{VH} of LDA at ~3100 cm^{-1} is confirmed. The χ''_{VH} profile seems to be different from that of vapor deposition amorphous solid water in which the existence of the characteristic mode around 3100 cm^{-1} cannot be clearly distinguished.[25] Since the $g_1(\nu)$ mode is extremely sensitive to the structure of hydrogen-bonded networks and the Raman profile of the LDA is similar to that of ice I$_h$, in which almost ideally tetrahedral hydrogen-bonded networks are formed, the existence of the $g_1(\nu)$ mode in the χ''_{VH} of LDA may associate with the topological order of hydrogen-bonded networks such as tetrahedrality of water. However, this speculation is not clarified yet and we expect the further Raman studies of LDA in future.

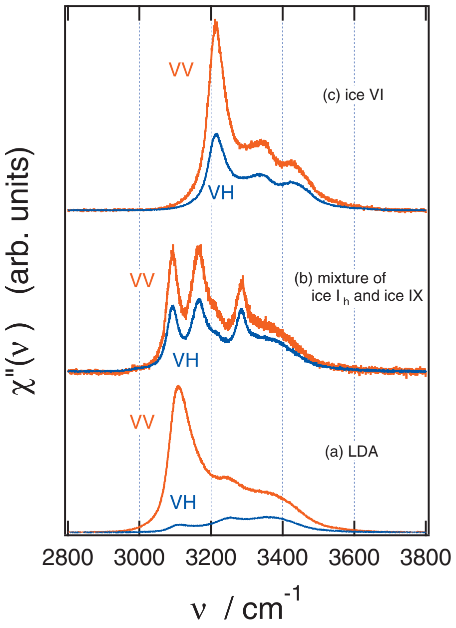

FIG. 5. Polarized (VV) reduced Raman spectra (red) and depolarized (VH) reduced Raman spectra (blue) for LDA and high-pressure crystalline ices in the OH-stretching region. (a) LDA made by heating the 1.5 GPa-relaxed HDA up to 120 K at 1 atm. (b) Mixture of ice I_h and XI made by heating the unannealed HDA up to 160 K at 0.2 GPa. (c) Ice VI made by heating the unannealed HDA up to 200 K at 1.5 GPa.

The polarized Raman spectra of high-pressure ices which are made by the crystallization of HDA at 0.2 GPa at 160 K and at 1.5 GPa at 200 K are shown in Figs. 5(b) and 5(c), respectively. By comparing of these Raman profiles with Raman profiles of various high-pressure crystalline ices,[26] the high-pressure ice made by the crystallization of HDA at 0.2 GPa is identified as a mixture of crystalline ice IX and I_h and the high-pressure ice made by the crystallization of HDA at 1.5 GPa is identified as crystalline ice VI. These identifications are consistent with the x-ray diffraction results reported by Salzmann *et al.*[20] It is found that there are some strong and some sharp peaks in the Raman spectra of these crystalline ices. Although the 0.2 GPa-relaxed and 1.5 GPa-relaxed HDA are annealed slightly below their T_x, their Raman profiles, particularly the χ''_{VH} profiles, have no sharp and no strong peaks which characterize crystalline ice and seem to be different from the Raman profile of LDA. Rather, these Raman profiles seem to be similar to that of liquid water. It has been reported that the low-frequency Raman spectra of the 1.5 GPa-relaxed HDA is broad and its profile is similar to a low-frequency Raman profile of liquid water.[27] These similarities between their Raman spectra suggest that HDA relates thermodynamically to liquid state.[27–31] In addition, this suggests that the inhomogeneously disordered structure in the unannealed HDA is irrelevant to crystalline structure such as high-pressure crystalline ice.[32–34] If crystalline ices such as an intermediate during the transition from ice I_h to high-pressure ices are hidden in the unannealed HDA, the distorted crystalline structure will be rearranged by annealing and then more perfect crystalline structure will be reconstructed and the crystalline phase will grow. As the result, the sharp and strong peaks relating to the crystalline phase should appear in the Raman spectra. However, there is no sharp peak in Raman spectra of the 0.2 GPa-relaxed and 1.5 GPa-relaxed HDA. This implies that there is no growth of crystalline ices in both the relaxed HDAs. Therefore, the nature of HDA is not nanosized crystalline ice but liquid.

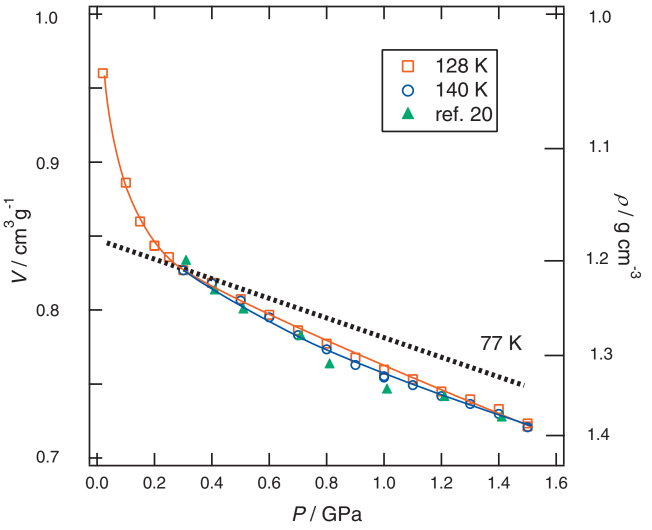

FIG. 6. *P-V* curves of the relaxed HDA. The volume of HDA at 128 (red squares) and 140 K (blue circles) are extracted from *T-V* curves in Fig. 1. A broken line represents the *P-V* curve of the unannealed HDA at 77 K. Solid curves are drawn to guide eye. Green triangles denote the volume of the relaxed HDA just before the T_x, which has been reported in Ref. 20.

Now, we plot values of the volume at 128 and 140 K, which are extracted from the *T-V* curves in Fig. 1, as a function of pressure in Fig. 6. According to the above discussion, the relaxed HDA at 128 and 140 K is regarded as HDA in the nearly equilibrium state. These values coincide with the results of Salzmann's works[20] within errors. Salzmann *et al.*[20] have reported that the sudden kink of volume change exists at 0.8 GPa and have stated that the HDA annealed above 0.8 GPa, which is corresponds to VHDA, is distinct from the HDA annealed below 0.8 GPa. To the contrary, there are some reports that the state of VHDA is an equilibrium state in which the HDA relaxed to be and VHDA and HDA belong to the same category.[19,35–37] The *P-V* curve at 128 K and the *P-V* curve at 140 K seem to be smooth and continuous in pressure range below 1.5 GPa, as shown in Fig. 6. It is not able to find the sudden kink in the *P-V* curve though the slope of the *P-V* curve becomes large below ~0.4 GPa. Considering that the χ''_{VV} and χ''_{VH} profiles of the 0.2 GPa-relaxed HDA resemble those of the 1.5 GPa-relaxed HDA, the annealed and expanded HDA at low pressure and the annealed and densified HDA at high pressure may belong to a same category. However, it is difficult to clarify whether there is the sudden kink of volume change at ~0.8 GPa or not. It may also be fitted similarity well by two lines intersecting close to 0.8 GPa.[20] We think it is necessary to study the more accurate state of the relaxed HDA further.

IV. CONCLUSION

We have measured the volume change of HDA on isobaric heating in a pressure range between 0.1 and 1.5 GPa and have measured the polarized Raman spectra of the unannealed HDA and of the relaxed HDA under pressure. A relatively strong $g_1(\nu)$ mode around 3100 cm^{-1} in the χ''_{VH} of unannealed HDA becomes small by annealing at low and high pressures. The χ''_{VH} profile of the relaxed HDA is similar to that of liquid water and glassy aqueous solution. This suggests that the relaxed HDA reaches the nearly equilibrium state and that the nature of HDA relates intrinsically to liquid. Moreover, although the stepwise *P*-*V* curve was observed on the isothermal compression of HDA,[12] the *P*-*V* curve of the HDA relaxed by isobaric heating seems to be smooth.

ACKNOWLEDGMENTS

We are grateful to O. Mishima for many helpful discussions.

[1] O. Mishima and H. E. Stanley, Nature (London) **396**, 329 (1998).
[2] P. G. Debenedetti, J. Phys.: Condens. Matter **15**, R1669 (2003).
[3] P. H. Poole, F. Sciortino, U. Essmann, and H. E. Stanley, Nature (London) **360**, 324 (1992).
[4] T. Loerting, C. Salzmann, I. Kohl, E. Mayer, and A. Hallbrucker, Phys. Chem. Chem. Phys. **3**, 5355 (2001).
[5] J. L. Finney, D. T. Bowron, A. K. Soper, T. Loerting, E. Mayer, and A. Hallbrucker, Phys. Rev. Lett. **89**, 205503 (2002).
[6] S. Klotz, Th. Strässle, M. A. Saitta, G. Rousse, G. Hamel, R. J. Nelmes, J. S. Loveday, and M. Guthrie, J. Phys.: Condens. Matter **17**, S967 (2005).
[7] C. G. Salzmann, T. Loerting, S. Klotz, P. W. Mirwald, A. Hallbrucker, and E. Mayer, Phys. Chem. Chem. Phys. **8**, 386 (2006).
[8] M. M. Koza, B. Geil, K. Winkel, C. Köhler, F. Czeschka, M. Scheuermann, H. Schober, and T. Hansen, Phys. Rev. Lett. **94**, 125506 (2005).
[9] M. M. Koza, Phys. Rev. B **78**, 064303 (2008).
[10] M. M. Koza, B. Geil, M. Scheuermann, H. Schober, G. Monaco, and H. Requardt, Phys. Rev. B **78**, 224301 (2008).
[11] M. M. Koza, T. Hansen, R. P. May, and H. Schober, J. Non-Cryst. Solids **352**, 4988 (2006).
[12] T. Loerting, W. Schustereder, K. Winkel, C. G. Salzmann, I. Kohl, and E. Mayer, Phys. Rev. Lett. **96**, 025702 (2006).
[13] R. J. Nelmes, J. S. Loveday, Th. Strässle, C. L. Bull, M. Guthrie, G. Hamel, and S. Klotz, Nat. Phys. **2**, 414 (2006).
[14] M. S. Elsaesser, K. Winkel, E. Mayer, and T. Loerting, Phys. Chem. Chem. Phys. **12**, 708 (2010).
[15] S. Klotz, Th. Strässle, R. J. Nelmes, J. S. Loveday, G. Hamel, G. Rousse, B. Canny, J. C. Chervin, and A. M. Saitta, Phys. Rev. Lett. **94**, 025506 (2005).
[16] C. A. Tulk, C. J. Benmore, J. Urquidi, D. D. Klug, J. Neuefeind, B. Tomberli, and P. A. Egelstaff, Science **297**, 1320 (2002).
[17] M. M. Koza, H. Schober, H. E. Fischer, T. Hansen, and F. Fujara, J. Phys.: Condens. Matter **15**, 321 (2003).
[18] O. Mishima and Y. Suzuki, Nature (London) **419**, 599 (2002).
[19] Y. Suzuki and O. Mishima, J. Phys.: Condens. Matter **21**, 155105 (2009).
[20] C. G. Salzmann, E. Mayer, and A. Hallbrucker, Phys. Chem. Chem. Phys. **6**, 5156 (2004).
[21] Y. Yoshimura, H. K. Mao, and R. J. Hemley, Chem. Phys. Lett. **420**, 503 (2006).
[22] R. J. Hemley, L. C. Chen, and H. K. Mao, Nature (London) **338**, 638 (1989).
[23] C. I. Ratcliffe and D. E. Irish, J. Phys. Chem. **86**, 4897 (1982).
[24] H. Hamaguchi, *Advances in Infrared and Raman Spectroscopy*, edited by R. J. H. Clark and R. E. Hester (Wiley, Heyden, 1985), Vol. 12, Chap. 6.
[25] J. P. Devlin, J. Chem. Phys. **90**, 1322 (1989).
[26] B. Minceva-Sukarova, W. F. Sherman, and G. R. Wilkinson, J. Phys. C **17**, 5833 (1984).
[27] Y. Suzuki, Y. Takasaki, T. Tominaga, and O. Mishima, Chem. Phys. Lett. **319**, 81 (2000).
[28] M.-C. Bellissent-Funel, Europhys. Lett. **42**, 161 (1998).
[29] J. F. Finney, A. Hallbrucker, I. Kohl, A. K. Soper, and D. T. Bowron, Phys. Rev. Lett. **88**, 225503 (2002).
[30] O. Mishima, Nature (London) **384**, 546 (1996).
[31] O. Mishima and Y. Suzuki, J. Chem. Phys. **115**, 4199 (2001).
[32] G. P. Johari, Phys. Chem. Chem. Phys. **2**, 1567 (2000).
[33] H. Schober, M. M. Koza, A. Tölle, C. Masciovecchio, F. Sette, and F. Fujara, Phys. Rev. Lett. **85**, 4100 (2000).
[34] M. M. Koza, R. P. May, and H. Schober, J. Appl. Crystallogr. **40**, s517 (2007).
[35] R. Martoňák, D. Donadio, and M. Parrinello, J. Chem. Phys. **122**, 134501 (2005).
[36] R. Martoňák, D. Donadio, and M. Parrinello, Phys. Rev. Lett. **92**, 225702 (2004).
[37] N. Giovambattista, H. E. Stanley, and F. Sciortino, Phys. Rev. Lett. **94**, 107803 (2005).